DOI: 10.36959/525/436 | Volume 1 | Issue 1

Current Trends in Analytical and Bioanlaytical Chemistry

Review Article Open Access

Cobalt Phthalocyanine Surface Acoustic Wave Sensor for Chloride Sensing in Water Samples

Najla Fourati[1]*, Chouki Zerrouki[1], Ajay Singh[2], Soumen Samanta[2] and Dinesh K Aswal[2,3]

[1]*SATIE, UMR CNRS, Cnam, Paris, France*

[2]*Technical Physics Division, Bhabha Atomic Research Center, Mumbai, India*

[3]*National Physical Laboratory, New Delhi, India*

Abstract

A 104 MHz Surface Acoustic Wave (SAW) sensor functionalized with a 100 nm thick Cobalt Phthalocyanine (CoPc) layer was investigated for chloride sensing in liquid media. Atomic force microscopy was first investigated to characterize the morphology of three phthalocyanine molecules, Pc, CoPc and FePc, deposited by molecular beam epitaxy on the SAW sensing area. CoPc was chosen for its particular columnar shape, highly suitable for sensing applications.

Gravimetric results indicate that the Limit of Detection (LOD) of the developed CoPc-SAW sensor was of order of 0.2 µM, and that the corresponding sensitivity was equal to (0.148 ± 0.001) °µM^{-1}. Recognition and release average time constants were estimated at (45 ± 7) s and (74 ± 4) s respectively.

Introduction

Chloride sensing is important in several fields such as environment or clinical diagnosis and for various industrial and chemical applications. Chloride ions are present in almost all natural waters, as they are leached from various rocks into soil and water by weathering. A World Health Organization (WHO) background document reported rivers chloride concentrations varying from 11-42 mg.L^{-1} in the United Kingdom, to 5-460 mg.L^{-1} in the USA, whereas those of contaminated wells in the Philippines are of about 141 mg.L^{-1} [1]. According to the WHO, chloride levels in unpolluted waters are often below 10 mg.L^{-1} and sometimes below 1 mg.L^{-1}.

Chloride ions are also the most abundant anion in human body. They are responsible for maintaining the acid-base balance of blood, the formation of hydrochloric acid in the stomach, transmitting nerve impulses, and regulating fluid in and out of cells [2]. Abnormal chloride concentrations in biological fluids (hypochloremia or hyperchloremia) may be related to various diseases such as metabolic or renal acidosis, congestive heart failure and metabolic alkalosis.

Besides, and because of their high mobility, chloride ions increase the electrical conductivity of water and therefore its corrosivity. According to WHO Regional Office for Europe [3], the presence of chloride in metal pipes increases levels of metals in drinking-water, as it reacts with them to form soluble salts, and enhances galvanic corrosion in lead pipes, despite the fact that a protective oxide layer is built up. Chloride ions can also interfere in concrete quality, as they can induce depassivation of the steel rebars and initiation of the corrosion process leading to degradation of the structure [4]. The costs of this corrosion are considerable and have led to the widespread use of chloride/water impermeable membranes on roadways and especially within bridges [5].

Several analytical techniques can be used to determine chloride concentration in water, including ion chromatography [6-8], near-infrared spectroscopy [9,10], and

***Corresponding author:** Najla Fourati, SATIE, UMR CNRS 8029, Cnam, 292 rue Saint Martin, 75003 Paris, France, Email: fourati@cnam.fr

Received: August 01, 2017: **Accepted:** September 27, 2017: **Published online:** September 29, 2017

Citation: Fourati N, Zerrouki C, Singh A, et al. (2017) Cobalt Phthalocyanine Surface Acoustic Wave Sensor for Chloride Sensing in Water Samples. Current Trends Anal Bioanal Chem 1(1):28-35

ion-selective electrodes [11,12]. Nowadays, research is focused on the development of chemical and biological sensors for chloride sensing. These devices present many advantages like high sensitivity, a relative ease of use, compactness, and a moderate cost per sample [13-15]. Chemical and biological sensors were developed for chloride detection inhuman fluids monitoring [16-21], civil infrastructure engineering [5,22-23], and environmental and industrial applications [4,24-30]. In all these cases, the transduction principle is either electrochemical or optical.

Here we report the use of a Surface Acoustic Wave sensors (SAW) sensor for chloride detection in aqueous solution. Functionalized with an appropriate sensing layer able to detect selectively the analyte of interest, SAW label free devices are robust, versatile and highly sensitive [31-34]. Their basic principle is related to the detection of changes in the propagation characteristics of surface acoustic waves generated by interdigital transducers on a given piezoelectric substrate.

For chloride detection, the SAW sensing area was functionalized with a thin layer of cobalt phthalocyanine. Several reasons have motivated this choice: i) Our "know how" in depositing thin layers of CoPc by molecular beam epitaxy, with a perfect control of both thickness and geometry of the zone on which the films are grown, ii) Their frequent use as recognition layers in chlorine gas sensors [35-37] and iii) Its particular columnar shape. To the best of our knowledge, this is the first study concerning chloride sensing with SAW sensors.

Here we demonstrate that CoPc based SAW sensors are able to detect chloride ions in liquid media, with a sub micromolar Limit of Detection (LOD). The Follow up of temporal variations of phase in both recognition and release processes permitted to estimate their time constants and thus to have an idea on their further reaction kinetics.

Chemicals and Instrumentation

Chemicals

Calcium Chloride ($CaCl_2$), Phthalocyanine (Pc), Cobalt Phthalocyanine (CoPc), Iron Phthalocyanine (FePc), H_2SO_4 (95%) and H_2O_2 (30%) were Purchased from Sigma Aldrich and were used as received.

SAW sensors functionalization by molecular beam epitaxy

Prior to investigated phthalocyanine films depositing, a piranha solution (1:1 (v/v) 98% H_2SO_4/30% H_2O_2) was dropped on the gold sensing area of the SAW sensors for 30 min in order to clean it and to activate the OH groups present onto the surface. Devices were then copiously rinsed with ultrapure water and immediately dipped in a methanol solution. SAW devices were after that dried using N_2 gas and loaded into the molecular beam epitaxy vacuum chamber (base vacuum ~ 2×10^{-8} mbar) for deposition of 100 nm thick films. The growth temperature and deposition rate were 50 °C and 2 Å.s^{-1} respectively.

Gravimetric measurement setup

The investigated SAW sensor consists of dual delay lines fabricated on a 36° rot Lithium Tantalate ($LiTaO_3$) piezoelectric substrate. The 20 nm Cr/80 nm Au thick Interdigital Transducers (IDTs) were designed with a periodicity of 40 µm (wavelength) which corresponds to an operating frequency of 104 MHz (Figure 1).

The measurement setup consists of a CoPc-SAW sensor, a Kalrez® flow cell deposited on the sensing area, a PMMA cover including Teflon inlets and outlets connected to a Gilson 3 peristaltic pump, and a home made pulse mode system (Figure 2).

The measured parameters were phase (at fixed frequency) and amplitude shifts of the sensing line according to the reference one [38]. The precise operating frequency is a

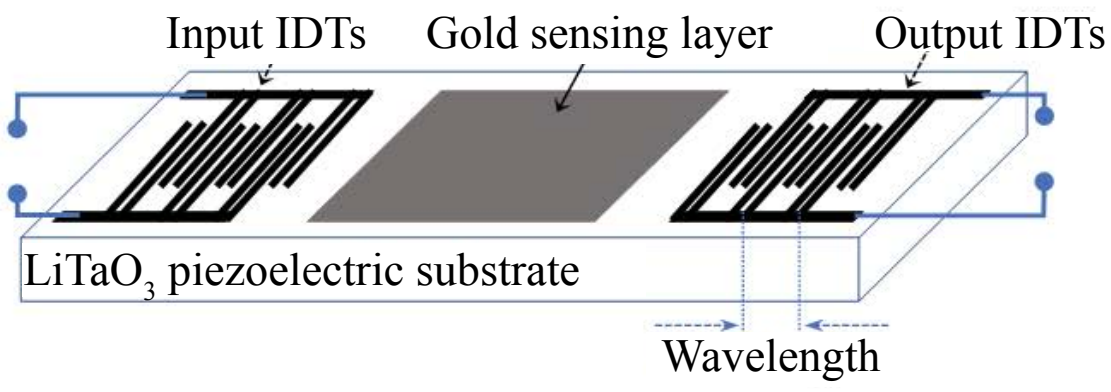

Figure 1: Schematic representation of a SAW delay line.

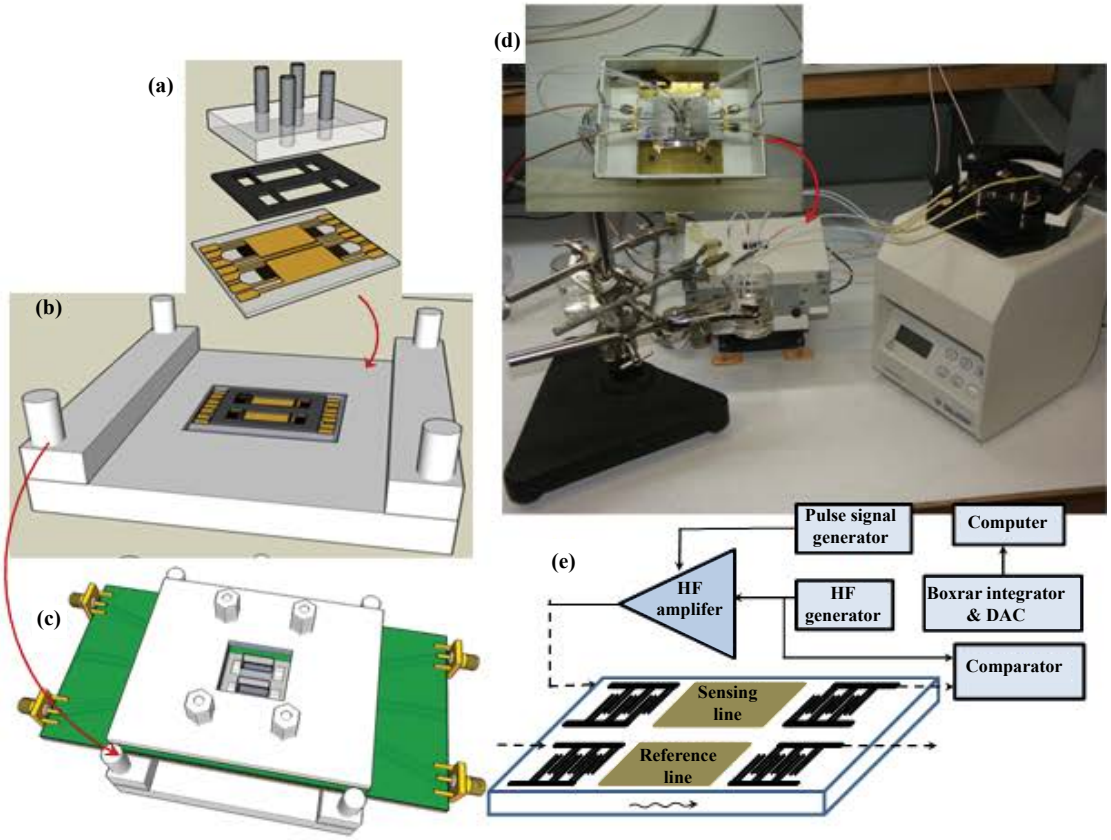

Figure 2: Schematic representation of the various parts of the sensing systems and overview of measurement system a) The dual delay lines SAW sensor and fluidic cell; b) The metallic base with SAW sensor; c) Overview of the system assembly with printed circuit board to access the electrical contacts and the metallic protection case; d) Overview of the system assembly and the fluidic circuit with peristaltic pump; e) Schematic diagram of the impulse mode system.

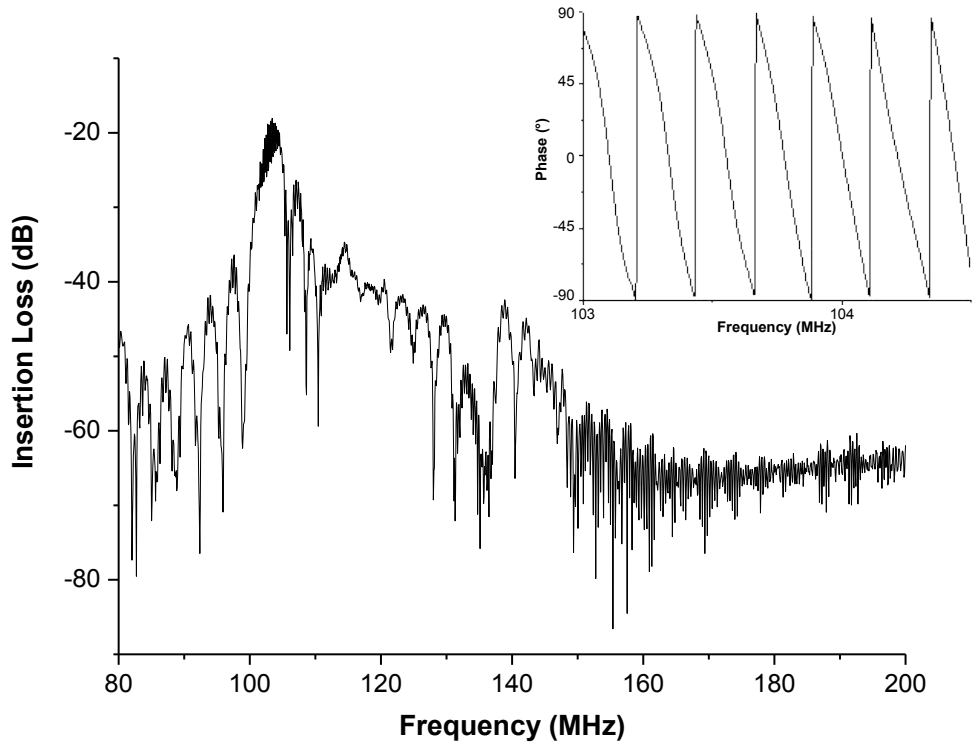

Figure 3: Frequency response of the SAW delay line. Inset: Output signal phase variation versus frequency around the operating frequency.

compromise between a linear output response (in the 101-104 MHz range) and a low insertion loss value. This permits to ensure that the output signal phase varies linearly during detection and that the amplitude signal does not fade during the recognition processes (Figure 3).

AFM measurements

AFM measurements were carried out under ambient conditions with a Nano surfeasy Scan 2 Flex system, in the phase contrast mode, equipped with commercially Tap190Al-G probes (from Budget Sensors). Cantilever's resonance frequency was of about 190 kHz and AFM probes curvature radius was inferior to 10 nm.

Results and Discussion

AFM morphological study for phthalocyanine film choice

Pc, FePc and CoPc films have been grown on gold sensing area of three SAW sensors. The corresponding photographies, presented in Figure 4, show varied colors which are related to differences in films thicknesses: 50 nm for one path and 100 nm for the other, for each SAW sensor. The best morphological performances were obtained with the 100 nm thick films which are considered herein.

Profiles made at the growth boundary permitted to estimate the step height at about (96.6 ± 1.9 nm), which is close to the expected 100 nm thick of Pc and metallic PC films (Figure 5).

Typical AFM images of SAW devices coated with Phthalocyanine (Pc) and Metalized ones (MPc, M is either Fe or Co) are presented in Figure 6. The (8 × 8) μm^2 images reveal a granular shape with regular distribution for the Pc film, and prominent grains, superposed to a granular back-ground for the MP cones. The limited size of explored zones, compared to that of sensing area

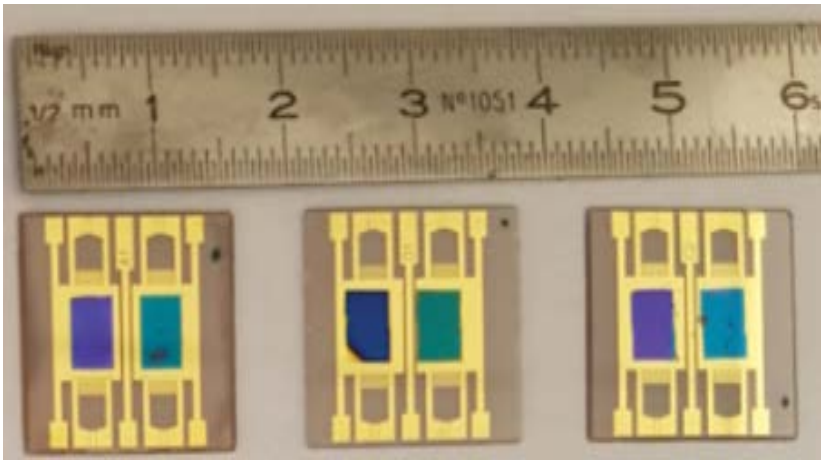

Figure 4: Photographies of three SAW sensors coated with: Pc (left), FePc (middle) and CoPc (right) film. Blue films are 100 nm thick, green ones are 50 nm thick.

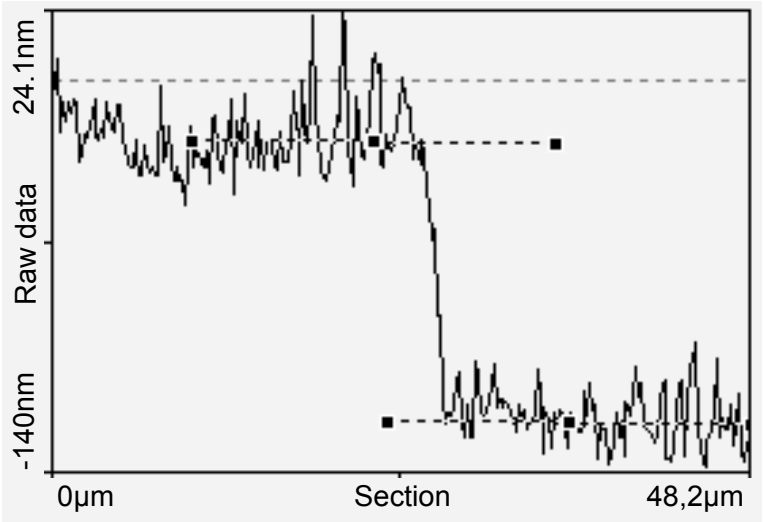

Figure 5: Profile of phtalocyanine film at the growth boundary.

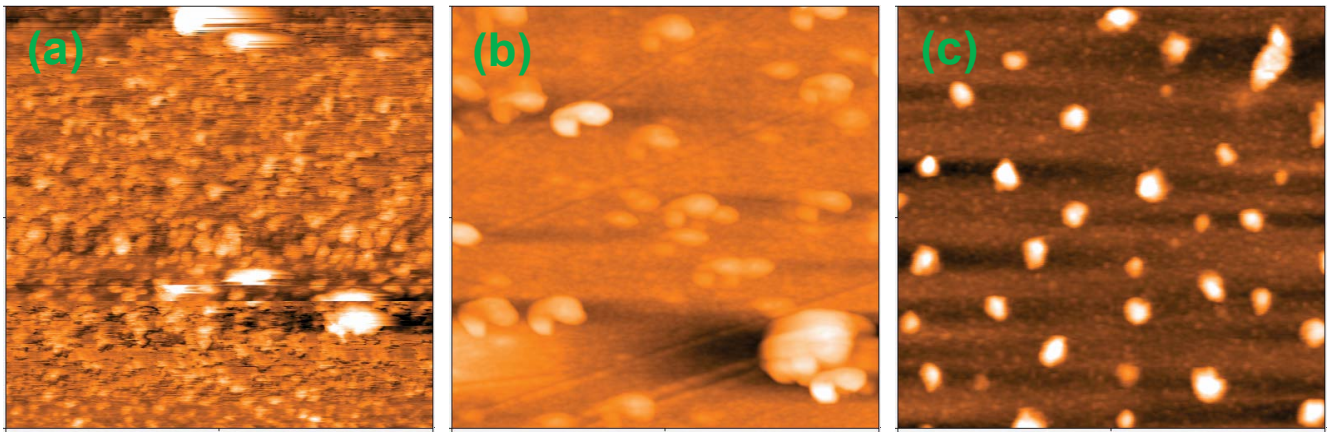

Figure 6: (8 × 8) μm² AFM images of phthalocyanine films deposited on gold surfaces a) Pc; b) FePc; c) CoPc.

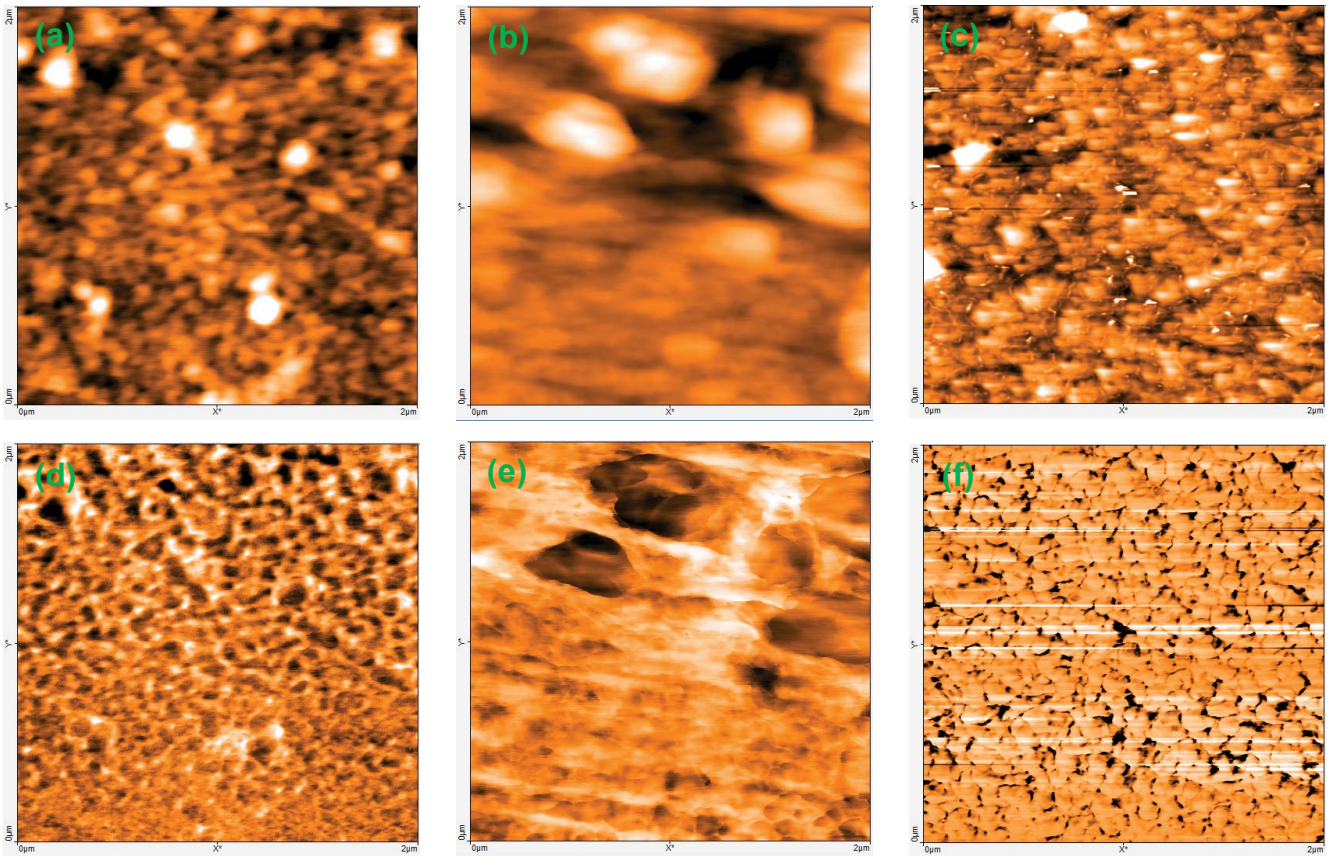

Figure 7: (2 × 2) μm² AFM images of Pc film. Topography: a) Pc; b; FePc, c) CoPc; Phase variation: d) Pc, e) FePc, f) CoPc.

which is of 2.5 × 8.5 mm², requires several measurements with accurate sampling to check possible differences according to the location. All the explored zones exhibited comparable aspects; the presented images are thus representative enough of the whole sensitive layer. For FePc, the protruding grains which are not uniformly distributed over the surface, present a slightly allonged shape with heights comprised between 39 nm and 107 nm. On the contrary, the regularly spaced grains are present over the entire surface in the case of CoPc film. Their corresponding height varies from 100 nm to 160 nm.

To highlight and quantify the differences between phthalocyanine films, and to minimize the effect of prominent grains for the metalized phthalocyanines, a smaller scan surface area of (2 × 2) μm² has been considered. We used the amplitude modulation mode imaging to access both topography and phase contrast, and thus complementary information (Figure 7).

Topographic and phase images highlight the difference between the three considered films. The CoPcone presents the most homogenous and regular surface, where the granular background exhibits dense structure

with high spatial frequencies asperities. At the opposite, FePc structure seems porous-like with inhomogeneous defects. From the topographic images, some statistical parameters have been extracted and gathered in Table 1. These values are representative, within uncertainties, of the entire sensitive surface, excepted the boundary regions. The Pc film is the smoothest one, with a rms roughness twice lower than those of FePc and CoPc. The latter presents the largest surface peak height S_p, confirming the fact that the CoPc film growths' process leads naturally to a columnar-like structure at different scales.

Table 1: Surface roughness parameters (in the spatial frequency range 0.5-256 μm^{-1}) of the three analyzed films: The root mean square height (rms roughness) S_q, the maximum surface peak height S_p and maximum surface valley depth S_v.

Surface roughness parameters (in nm)			
Phthalocyanine films	**S_q**	**S_p**	**S_v**
Pc	1.8 ± 0.2	13.2 ± 1.1	-5.3 ± 0.4
FePc	3.9 ± 0.3	13.5 ± 1.2	-12.5 ± 1.2
CoPc	4.1 ± 0.3	42.0 ± 2.7	-14.9 ± 1.2

According to all these results, and mainly due to the particular shape of CoPc film, which exhibits high developed surface suitable for sensing applications, we have chosen it for chloride sensing in aqueous media.

Gravimetric sensing of chloride in aqueous media

Chloride sensing by CoPc-SAW sensor has been investigated by recording phase variation versus time, after the injection of a given concentration of Cl^- ions in the 10^{-6}-10^{-2} M range (Figure 8a). In addition to the use of a

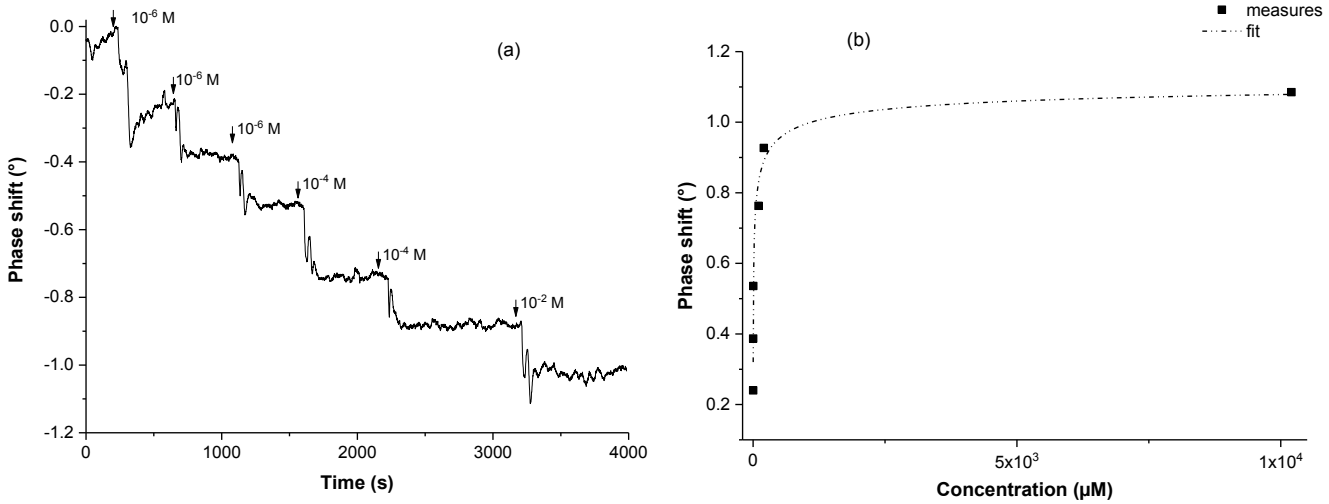

Figure 8: Gravimetric response of the CoPc-SAW sensors for chloride solutions a) Phase shift versus time after injection of solutions with different concentrations; b) Cumulative phase shifts according to chloride concentration.

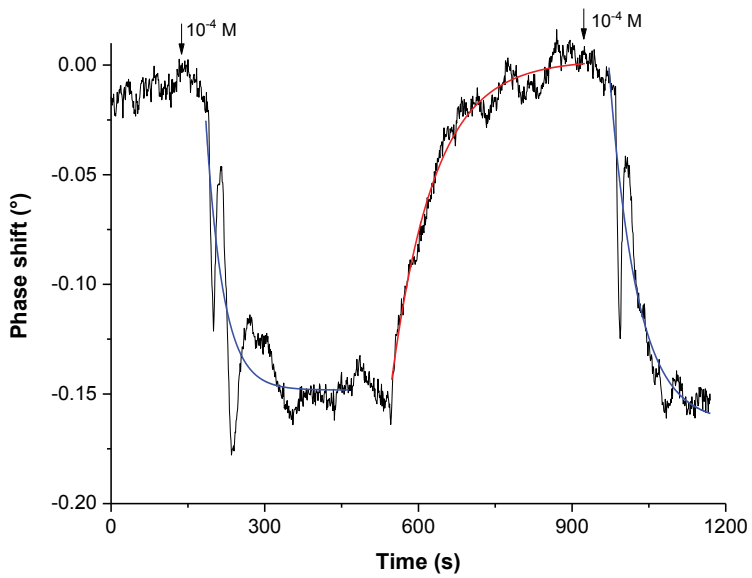

Figure 9: Recognition and release of chloride by the CoPc/SAW sensors. Phase variation versus time and exponential growth and decay models.

dual delay-lines configuration with reference and sensing paths, all the investigated solutions (deionized water and chloride solutions) were kept at room temperature, close to the measurement system. This procedure permits to avoid any temperature variation influence during solutions injection or in the detection process. Thus, the decreases of the output signal phase after chloride ions injections indicate the evidence of their further recognition by the CoPc layer.

The follow up of phase shifts according to analyte concentration, presented in (Figure 8b), shows a general power-law variation, with a quasi-linear response in the micromolar range.

The saturation value of the CoPC-SAW sensor was of order of 5.10^{-4} M. The Limit of Detection (LOD) is dependent on the stability of the system, namely, the fluctuation in the output of the sensor in absence of the analyte of interest. In our case, the standard deviation σ of the sensor output signal is of order of 0.007°. The minimum measurable signal is often estimated at 3σ (0.02°), the LOD was thus estimated at 0.2 μM. This value is comparable to that obtained by Bujes-Garrido, et al. [24] and L Trnkova [4], who have investigated electrochemical sensors for chloride detection, and largely inferior to that estimated by Kim, et al. [16]. Sensitivity of the developed sensor was of order of (0.148 ± 0.001) °μM^{-1}.

Several consecutive recognitions, separated by a recovery were then considered to determine the recognition kinetic of the chlorides by the CoPC film. For the recovery step, DI water was pumped, at a constant flow rate of 0.19 ml. min^{-1}, over the SAW sensing area to "extract" and evacuate the investigated analyte. To have sufficient magnification to illustrate the concordance between the experience and the fits from which time constants will be extracted the, only one recognition-release cycle has been presented (Figure 9). Phase variations versus time were adjusted with exponential decay and exponential growth functions for recognition and release processes respectively. Fit parameters permitted to estimate the time constants: (37 ± 3) s and (53 ± 5) s for the first and the second chloride recognitions and (74 ± 2) s for its release.

The fitting of all experiments of chloride recognitions and releases, indicates that the reactions kinetics are independent on the analyte concentration. However, the average time constants values, (45 ± 7) s for recognitions and (74 ± 4) s for releases, indicate that the first is roughly twice faster than the second one.

We think that the presence of damped oscillations at the end of the recognition processes can be related to a local structure reconfiguration which occurs around the recognitions sites. The absence of similar effects in the release process is probably due to its relative slowness.

Conclusion

A 104 MHz surface acoustic wave sensor coated with a 100 nm thick layer of cobalt phthalocyanine was designed for chloride sensing in liquid media. CoPc was chosen among other phthalocyanine molecules (Pc and FePc) due to its particular morphology, which makes it suitable for sensing applications. Gravimetric results show that the CoPc-SAW sensor has a detection limit of order of 0.2 μM. The corresponding sensitivity was estimated at (0.148 ± 0.001) °μM^{-1}.

Investigating SAW sensors in particular and piezoelectric devices in general, can thus be envisaged as a new route for ions detection in aqueous media. The key parameters remain the choice of a judicious sensing layer and the precise control of its structure and topography.

References

1. http://www.who.int/water_sanitation_health/dwq/chloride.pdf
2. http://www.rsc.org/Education/Teachers/Resources/cfb/inorganicions.htm
3. WHO Regional Office for Europe (1979) Sodium, chlorides, and conductivity in drinking-water: A report on a WHO working group, The Hague 1-5 May 1978. Euro reports and studies. World Health Organization Regional Office for Europe, Copenhagen, Denmark.
4. L Trnkova, Adam V, Hubalek J, et al. (2008) Amperometric Sensor for Detection of Chloride Ions. Sensors 8: 5619-5636.
5. PL Fuhr, Brian D MacCraith, Dryver R Huston, et al. (1997) Fiber optic chloride sensing: If corrosion's the problem, chloride sensing is the key. Proceedings of SPIE-The International Society for Optical Engineering, Fiber Optic Sensor Workshop, 92-104.
6. JS Pereiraa, Diehl LO, Duarte FA, et al. (2008) Chloride determination by ion chromatography in petroleum coke after digestion by microwave-induced combustion. J Chromatogr A 1213: 249-252.
7. JB Xiao (2006) Determination of nine components in Bayer liquors by high performance ion chromatography with conductivity detector. J Chil Chem Soc 51: 964-967.
8. JA Morales, de Graterol LS, Mesa J (2000) Determination of chloride, sulfate and nitrate in groundwater samples by ion chromatography. J Chromatogr A 884: 185-190.
9. RH Wu, XG Shao (2006) Application of near-infrared spectra in the determination of water soluble chloride ion in plant samples. Guang Pu Xue Yu Guang Pu Fen Xi 26: 617-619.
10. TH Begley, Elaine Lanza, Karl H Norris, et al. (1984) Determination of sodium chloride in meat by near-infrared diffuse reflectance spectroscopy. J Agric Food Chem 32: 984-987.
11. FL Cerklewski, JW Ridlington (1987) Chloride determination in foods with ion-selective electrode after isolation as hydrogen chloride. J Assoc Off Anal Chem 70: 924-926.
12. A Bratovcic, A Odobasic (2011) Determination of Fluoride and Chloride Contents in Drinking Water by Ion Selective Electrode. Environmental Monitoring.
13. G Zanchetta, R Lanfranco, F Giavazzi, et al. (2017) Emerg-

ing applications of label-free optical biosensors. Nanophotonics 6: 627-645.

14. J Nimisha, J Rajeev, S Swati, et al. (2016) Recent trends in electrochemical sensors for multianalyte detection - A review. Talanta 161: 894-916.
15. A Sobczak-Kupiec, Jayachandran Venkatesan, Adnan Alhathal AlAnezi, et al. (2016) Magnetic nanomaterials and sensors for biological detection. Nanomedicine 12: 2459-2473.
16. JP Kim, Zhiwei Xie, Michael Creer, et al. (2017) Citrate-based fluorescent materials for low-cost chloride sensing in the diagnosis of cystic fibrosis. Chemical Science 8: 550-558.
17. VAT Dam, MAG Zevenbergen, R van Schaijk (2015) Flexible chloride sensor for sweat analysis. Procedia Engineering 120: 237-240.
18. S Zhong, N Dhasakumar, Joseph Santos-Sacchi (2014) A Genetically-Encoded YFP Sensor with Enhanced Chloride Sensitivity, Photostability and Reduced Ph Interference Demonstrates Augmented Transmembrane Chloride Movement by Gerbil Prestin (SLC26a5). PLoS One 9: e99095.
19. P Bregestovski, D Arosio (2012) Green fluorescent protein-based chloride ion sensors for in vivo imaging. G Jung, Fluorescent Proteins II. Springer Ser Fluoresc 12: 99-124.
20. B Schazmann, D Diamond (2006) A chloride selective calix[4]arene optical sensor combining urea functionality with pyrene excimer transduction. Journal of the American Chemical Society 128: 8607-8614.
21. JH Shin, Hyo Lin Lee, Sung Ho Cho, et al. (2004) Characterization of epoxy resin-based anion-responsive polymers: Applicability to chloride sensing in physiological samples. Anal Chem 76: 4217-4222.
22. Subbiah Karthick, Seung-Jun Kwon, Han Seung Lee, et al. (2017) Fabrication and evaluation of a highly durable and reliable chloride monitoring sensor for civil infrastructure. RSC Advances 7: 31252-31263.
23. F Pargar, DA Koleva, EAB Koenders, et al. (2015) Monitoring the Electrochemical Response of Chloride Sensors Embedded in Cement Paste. Mater Res Soc Symp Proc.
24. J Bujes-Garrido, MJ Arcos-Martinez (2017) Development of a wearable electrochemical sensor for voltammetricdetermination of chloride ions. Sensors and Actuators B: Chemical 240: 224-228.
25. Julia Bujes-Garrido, M Julia Arcos-Martinez (2016) Disposable sensor for electrochemical determination of chloride ions. Talanta 155: 153-157.
26. H Cao, D HuiWu (2008) Rapid and Sensitive Determination of Trace Chloride Ion in Drinks Using Resonance Light Scattering Techniqu. Journal of Automated Methods and Management in Chemistry 2008: 745636.
27. CMG dos Santos, Thomas McCabe, Thorfinnur Gunnlaugsson (2007) Selective fluorescent sensing of chlorid. Tetrahedron Letters 48: 3135-3139.
28. N Durgesh, Tarlok Singh Lobana, Rakesh Kumar Mahajan (2009) Investigation of Chloride Ion-Sensing Property of Polymeric Membrane and Coated Graphite Sensors Based on Bis (furan-2-carbaldehyde-N-methylthiosemicarbazonato) nickel(II) Complex. Analytical Letters 42: 2474-2484.
29. Ying Zhang, Mei Xian Liu, Meng Yuan Lü, et al. (2005) Anion Chelation-Induced Porphyrin Protonation and Its Application for Chloride Anion Sensing. J Phys Chem A 109: 7442-7448.
30. Yan Bai, Bing-Guang Zhanga, Jian Xu, et al. (2005) Conformational switching fluorescent chemosensor for chloride anion. New Journal of Chemistry 29: 777-779.
31. N Ktari, N Fourati, C Zerrouki, et al. (2015) Design of a polypyrrole MIP-SAW sensor for selective detection of flumequine in aqueous media. Correlation between experimental results and DFT calculations. RSC Adv 5: 88666-88674.
32. Naima Maouche, Nadia Ktari, Idriss Bakas (2015) A surface acoustic wave sensor functionalized with a polypyrrole molecularly imprinted polymer for selective dopamine detection. Journal of Molecular Recognition 28: 667-678.
33. Najla Fourati, Mahamadou Seydou, Chouki Zerrouki, et al. (2014) Ultrasensitive and Selective Detection of Dopamine Using Cobalt-Phthalocyanine Nanopillar-Based Surface Acoustic Wave Sensor. ACS Appl Mater Interfaces 6: 22378-22386.
34. N Fourati, C Zerrouki (2014) Immunosensing with surface acoustic wave sensors: toward highly sensitive and selective improved piezoelectric biosensors. In: Jean-Hugh Thomas, Nourdin Yaakoubi, New Sensors and Processing Chain. Wiley-ISTE.
35. Arvind Kumar, Soumen Samanta, S Latha, et al. (2017) Enhanced Cl_2 sensitivity of cobalt-phthalocyanine film by utilizing a porous nanostructured surface fabricated on glass. RSC Adv 7: 4135-4143.
36. Soumen Samanta, Arvind Kumar, Ajay Singh, et al. (2012) Influence of adsorbed oxygen on charge transport and chlorine gas-sensing characteristics of thin cobalt phthalocyanine films. Chemical Papers 66: 484-491.
37. AK Debnath, S Samanta, Ajay Singh, et al. (2009) Parts-per-billion level chlorine sensors with fast kinetics using ultrathin cobalt phthalocyanine films. Chemical Physics Letters 480: 185-188.
38. Y Bergaoui, C Zerrouki, N Fourati, et al. (2011) Antigen-antibody selective recognition using $LiTaO_3$ SH-SAW sensors: investigations on macromolecules effects on binding kinetic constants. Eur Phys J Appl Phys 56: 13705.